

Transmission properties of periodically patterned triangular prisms

Xiaojun Tian, Yongkai Wang, Liang Cao, Zhongyue Zhang*

School of Physics and Information Technology, Shaanxi Normal University, Xi'an 710062, China

Received 1 May 2014; received in revised form 30 July 2014; accepted 1 September 2014

Available online 22 September 2014

Abstract

Transmission properties of plasmonic structure arrays are simulated by finite element method. The array unit is composed of two combined triangular prisms. Results reveal that several resonant modes are found in the transmission spectra, which are due to the resonance of the surface plasmon polariton in the metal slit or to the localized surface plasmon resonance of the combined prisms. The resonant wavelengths can be tuned by changing the structural parameters of the combined prisms. In addition, the resonant modes are sensitive to small refractive index changes of the surrounding media, revealing potential detection applications in nanophotonic systems.

© 2014 Elsevier B.V. All rights reserved.

Keywords: Plasmonics; Surface plasmon polariton (SPP); Localized surface plasmon (LSP)

1. Introduction

Surface plasmons (SPs) are surface electromagnetic waves coupled with collective oscillation of electrons at metal/dielectric interfaces [1–3,12]. Two kinds of SPs are mainly found, namely localized surface plasmon (LSP) and surface plasmon polariton (SPP).

LSPs are charge density oscillations confined to the metallic nanostructures [4]. LSP resonant wavelength and electric field distribution are strongly dependent on the shape, size, and elements of the metal structures [5], making tuning the resonant wavelength and varying the electric field distribution possible by altering the metal structure. In addition, the resonant wavelength depends on the environment of the surrounding media [5], which has drawn much attention in sensor

applications using nanostructures with different topologies or different arrangement, such as nanospheres [6–9], nanodisks with missing wedge-shaped slices [10], dolmen nanostructures [11], and array of gold nanorods [12]. According to other research reports, the figure of merit (FoM) [13] ($\text{FoM} = (1/fwhm) \times (\Delta\omega/\Delta n)$, where $fwhm$ is the full width at half maximum, $\Delta\omega$ and Δn represent the variation of frequency and refractive index, respectively) of a single silver nanocube on dielectric substrate can reach 5.4 [13]. At optimized conditions, which formed a Fano resonance in the nanocube, it can produce a higher FoM ranging from 12 to 20 [14].

SPPs are generated by the resonant interaction between surface charge oscillation and the electromagnetic field of light, which decays exponentially in the perpendicular direction [15,16]. SPPs are tightly bound to the vicinity of the surface beyond the diffractive limit, implying the possibility of guiding light on the sub-micron scale [17], which raises tremendous interest in waveguide applications. The propagation properties of

* Corresponding author. Tel.: +86 187 10 39 08 97.

E-mail address: zyzhang@snnu.edu.cn (Z. Zhang).

SPPs have close connection with the structure parameters and the surrounding environment, which can also be used for sensor applications [18–25]. For a previous study, individual plasmonic structures are used to detect the refractive index changes in the resonator [20]. The FoM of SPP based sensor at metal/nematic liquid–crystal interface can reach 35 [26], and on the gold films, it can reach 54 [27], which exhibits a higher FoM than LSP sensor. However, the SPP intensity transmitted through the resonator is relatively weak. By contrast, the energy is strongly dependent on the excitation wave polarization in the SPP sensor application. All the above mentioned defects limit SPP sensors usage.

In the present paper, we propose a plasmonic sensor based on SPPs: it is composed of a periodic array of two combined triangular prisms. The triangular prisms are open to the outside media at two ends. In our calculations, the transmission characteristics of the structure are investigated through finite element method (FEM). Results show that several electron oscillation modes are found in the transmission spectra. These modes are caused by the resonance of the SPP propagation in the metal slit and the LSP of the combined prisms. In addition, the effects of structural parameters and dielectric media of the surrounding environment on their transmission properties are also studied. The results show very promising prospects of periodic triangular prism array for dielectric media sensor applications.

2. Structure and computational methods

Fig. 1 shows the plasmonic structure array and the unit of the periodic structure which is composed of two combined square triangular prisms placed in parallel.

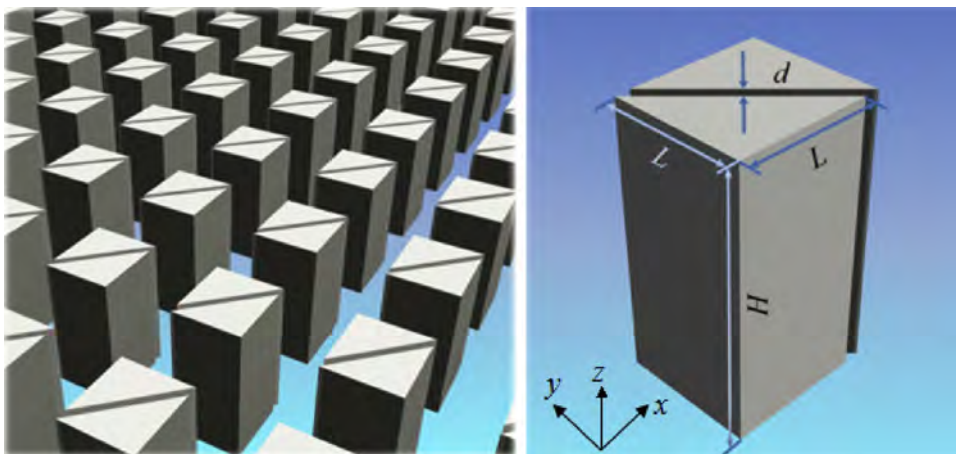


Fig. 1. Schematic diagram for the plasmonic structure composed of two triangular prisms with slit width of d , triangular side length of L , and height of H .

The prism has a height of H and a side length of L . The separation between two prisms is d . The periods in the x -direction and y -direction are both 200 nm. The incident light propagates along the z -direction with a polarization in the x -direction to excite the SPs around the prisms.

The transmission properties of the plasmonic structure arrays are investigated using a three-dimensional commercial FEM software (COMSOL Multiphysics). The frequency-dependent complex relative permittivity ε of silver has been presented by a previous paper in 1972 [28].

For metal–insulator–metal slit, the dispersion equation is characterized by [29,30]:

$$\tanh(\kappa d) = \frac{-2\kappa p\alpha}{\kappa^2 + p^2\alpha^2} \quad (1)$$

where κ and d are the perpendicular core wave vector and width of the insulator in the metal slit, respectively. The symbols in Eq. (1) are defined as $p = \varepsilon_{\text{in}}/\varepsilon_{\text{m}}$ and $\alpha_c = [k_0^2(\varepsilon_{\text{in}} - \varepsilon_{\text{m}}) + \kappa^2]^{1/2}$. ε_{in} and ε_{m} are the dielectric constants of the insulator and the metal, respectively. $k_0 = 2\pi/\lambda_0$ is the free space wave vector. κ can be solved from Eq. (1) by using the iterative method [20]. Thus, the effective index n_{eff} of the metal slit can be solved from $n_{\text{eff}} = [\varepsilon_{\text{m}} + (\kappa/k_0)^2]^{1/2}$. And the wavelength of SPPs can be expressed as $\lambda_{\text{spp}} = \lambda_0/\text{Re}(n_{\text{eff}})$, where $\text{Re}(n_{\text{eff}})$ is the real part of n_{eff} .

3. Results and discussion

Fig. 2 shows the transmission spectra of the combined triangular prism array and the cubic array. The slit width, side length, and vertical height of the prism are 10 nm, 100 nm, and 200 nm, respectively. As shown in Fig. 2,

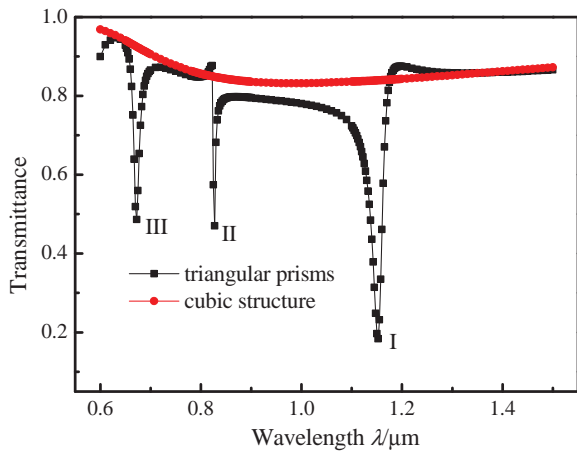


Fig. 2. Transmission spectra of the plasmonic structure with slit width $d=10$ nm, side length $L=100$ nm, and structure height $H=200$ nm compared with the cubic structure with the same L and H .

three valleys appear at $\lambda_I=1.15$ μm , $\lambda_{II}=0.83$ μm , and $\lambda_{III}=0.67$ μm , respectively. Compared with the cubic array, no valleys are noted in the transmission spectrum.

To illustrate the nature of these resonant modes in Fig. 2, the electric field distributions at these wavelengths are calculated. As shown in Fig. 3, at $\lambda_I=1.15$ μm , large electric fields distribute at the two ends of the slit. At $\lambda_{III}=0.67$ μm , large electric fields distribute at the two ends and the middle of the slit. When the SPPs are coupled into the slit, they propagate along the slit and can be reflected back at the ends. The slit can be regarded as a metal–insulator–metal waveguide and the slit composed by the adjacent prisms can be treated as a resonator for SPPs. The resonant condition for the cavity is:

$$H = \frac{N\lambda_{\text{spp}}}{2} = \frac{N(\lambda/Re(n_{\text{eff}}))}{2} \quad N = 1, 2, 3, \dots \quad (2)$$

In our study, $H=200$ nm. Using the method described previously, at $\lambda_I=1.15$ μm and $\lambda_{III}=0.67$ μm , the wavelength of SPPs in the slit is $\lambda_{I\text{spp}}=0.487$ μm and $\lambda_{III\text{spp}}=0.266$ μm , respectively. The corresponding N is $N_I \approx 1$ and $N_{III} \approx 2$, which are consistent with the electric field distribution in Fig. 3. At $\lambda_{II}=0.83$ μm , the enhanced electric field is located outside the slit at y -direction, which is mainly caused by the LSP resonance.

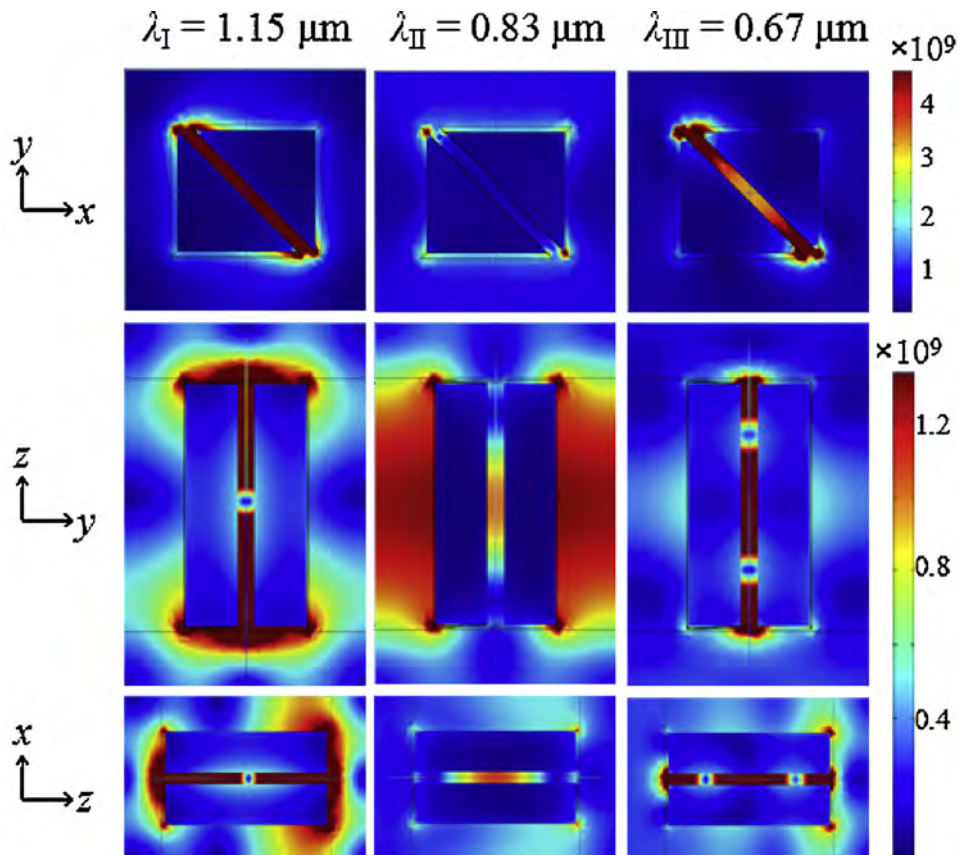


Fig. 3. Electric field distributions of the plasmonic structure at resonant wavelengths of $\lambda_I=1.15$ μm , $\lambda_{II}=0.83$ μm , and $\lambda_{III}=0.67$ μm .

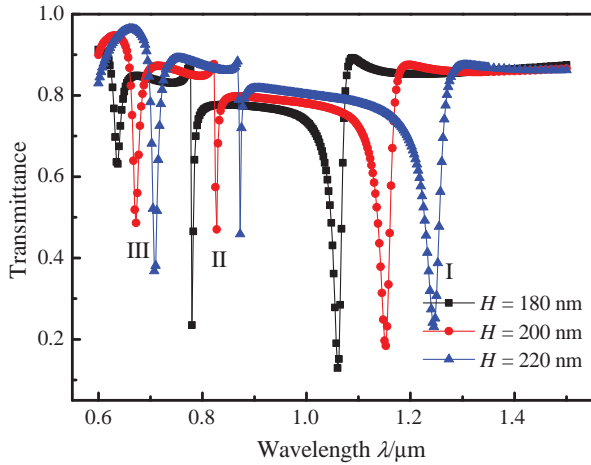


Fig. 4. Transmission spectra of the plasmonic structure with various heights H at $d = 10$ nm and $L = 100$ nm.

Nanostructures are usually irradiated to produce LSP. In our study, two adjacent prisms form a slit. When the two combined prism arrays are irradiated by plane waves, SPP resonant modes appear in the transmission spectra.

To investigate the effects of structural parameters on the plasmonic structure array transmission spectra, the dimensions of the structure are varied systematically. First, H is noted at 180 nm, 200 nm and 220 nm with fixed $d = 10$ nm and $L = 100$ nm. As shown in Fig. 4, for different H s, the shape of the transmission spectra are similar. With increased H , the whole transmission spectra experience a red shift. The reason for this phenomenon is that for the same mode, the values of N are the same, and the resonant wavelength of SPPs increases with increased H , which results in the red shift of the excitation wavelength λ .

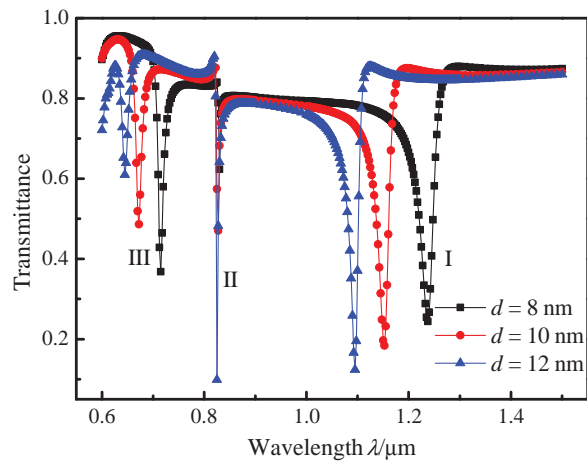


Fig. 5. Transmission spectra of the plasmonic structure with various slit widths d at $L = 100$ nm and $H = 200$ nm.

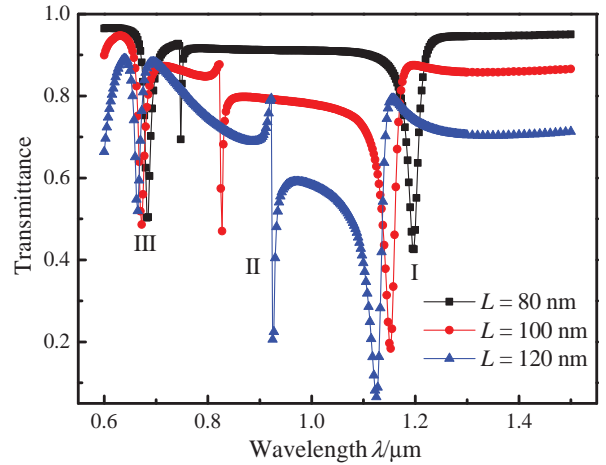


Fig. 6. Transmission spectra of the plasmonic structure with various side lengths L at $d = 10$ nm and $H = 200$ nm.

The effect of slit width d is studied by obtaining its values at 8 nm, 10 nm, and 12 nm with fixed $L = 100$ nm and $H = 200$ nm. Fig. 5 illustrates the transmission spectra of the plasmonic structure. For modes I and III, the resonant wavelengths blue shift to a shorter wavelength with increased d . When both N and H are fixed, the resonant wavelength of SPPs remains unchanged with different d s. However, the excitation wavelength decreases according to Eq. (2). Mode II is mainly caused by the LSP of the prism and it shifts unnoticeably with increased d .

The effect of side length L has also been investigated by obtaining its values at 80 nm, 100 nm, and 120 nm with fixed $d = 10$ nm and $H = 200$ nm. As shown in Fig. 6, resonant modes I and III experience a blue shift and mode II experiences a red shift with increased L . With

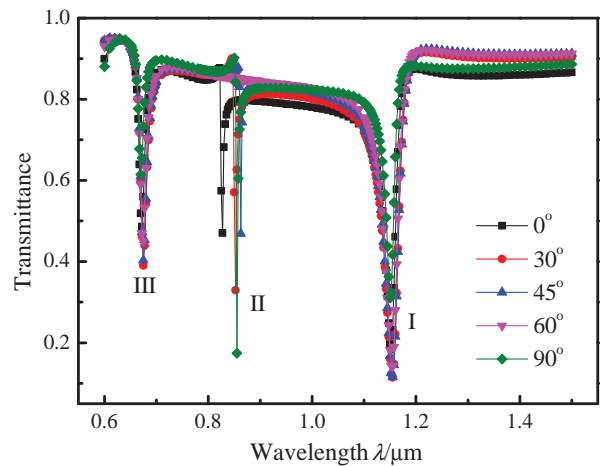


Fig. 7. Transmission spectra of the plasmonic structure with different polarization directions at $d = 10$ nm, $L = 100$ nm, and $H = 200$ nm.

increased L , the limiting effect of the two combined prisms increases, which then decreases the SPP wavelength in the slit. Such change results in the blue shift of the resonant wavelength. With increased L , the electron oscillation length increases, which results in the red shift of mode II.

In addition, due to the structure asymmetry, we calculated the transmission spectra with different polarizations that range from 0° to 90° with fixed $L = 100$ nm, $d = 10$ nm, and $H = 200$ nm. As shown in Fig. 7, resonant modes I and III are not shifted, and mode II shifts slightly. The results indicate that the plasmonic structure is not sensitive to the polarization direction of incident light, which extends its sensor applications.

For the demonstration of the plasmonic structure sensitivity to the surrounding media, we investigated

the effect of different refractive indexes of surrounding media on the transmission spectra, as shown in Fig. 8(a). The slit width, side length of the triangle, and the height of the structure are 10 nm, 100 nm and 200 nm, respectively. The incident light beam polarizes in the x -direction. When the structure is immersed in some fluid media with refractive index n , as shown in Fig. 8(b), the wavelengths of the valleys red shift with increased n . The resonant wavelengths show a linear relationship with n (not shown in this paper), and the refractive index (RI) sensitivity (noted with S) of these modes are $S_I = 1110$ nm/RIU, $S_{II} = 778$ nm/RIU, and $S_{III} = 611$ nm/RIU. On the other hand, the full width at half maximum ($fwhm$, with the unit of “eV”) of three modes are $fwhm_I = 0.027$, $fwhm_{II} = 0.021$, and $fwhm_{III} = 0.041$, respectively. And the ratios of

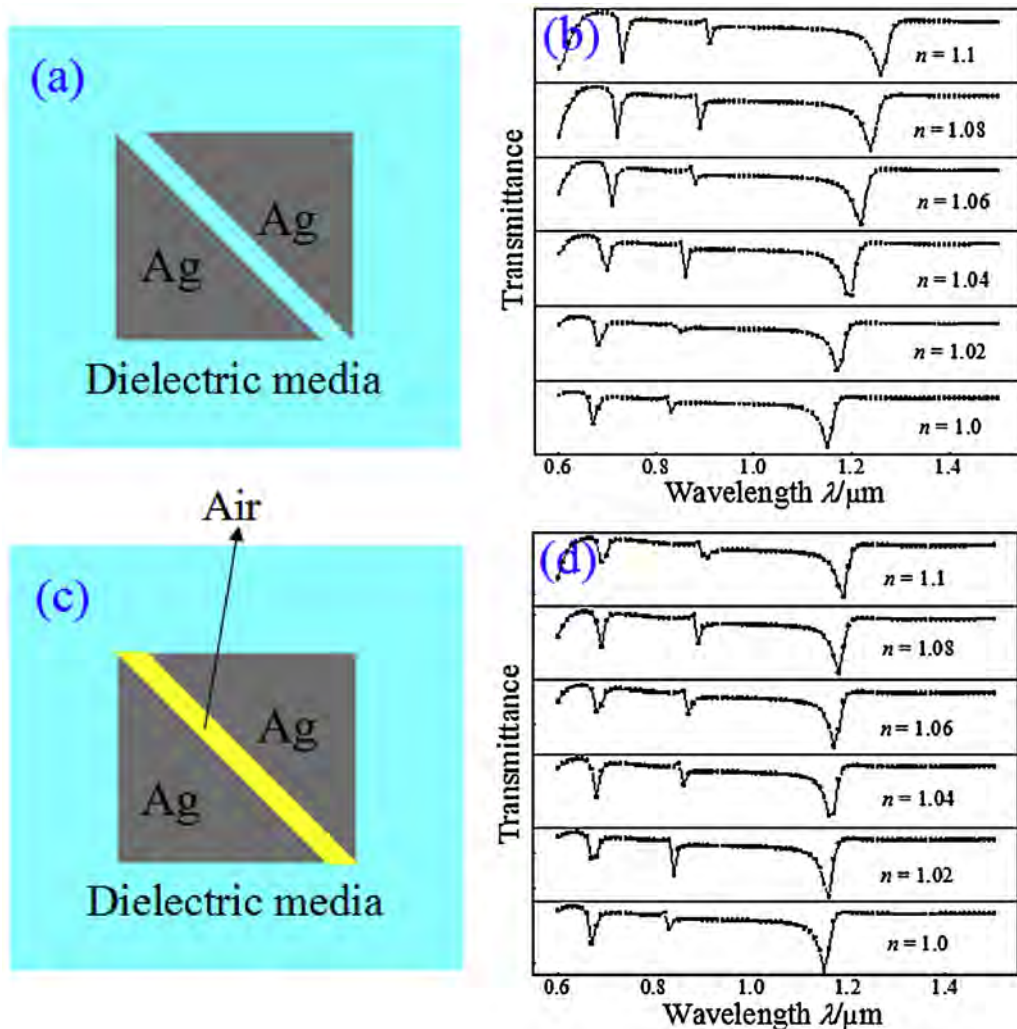


Fig. 8. (a) The schematic of the structure filled by various dielectric media with different refractive index n . (b) Transmission spectra of the plasmonic structure corresponding to (a). (c) The schematic of the structure with air into the slit, and different dielectric media outside the slit. (d) Transmission spectra of the plasmonic structure corresponding to (c).

frequency variation to refractive index variation at the three resonant modes are $\Delta\omega_I/\Delta n_I = 0.96$, $\Delta\omega_{II}/\Delta n_{II} = 1.41$, and $\Delta\omega_{III}/\Delta n_{III} = 1.70$, respectively. Thus, the FoMs of the three modes are $\text{FoM}_I = 36.06$, $\text{FoM}_{II} = 68.80$, and $\text{FoM}_{III} = 41.46$. As previous discussed, the resonant modes I and III are not sensitive to the incident polarization. The resonant wavelength shifts of modes I and III as incident polarization varies from 0° to 90° are equivalent changes in environmental RIU of 0.0045 and 0.0082, respectively. In addition, since the width of slit is small (~ 10 nm), air would keep inside the slits when the structure immersed in fluid media, as shown in Fig. 8(c). Fig. 8(d) shows the transmission spectra of the plasmonic structure with surrounding conditions of Fig. 8(c). Three resonant modes also experience a red shift with increased n and sensitivities are $S_I = 389$ nm/RIU, $S_{II} = 778$ nm/RIU, and $S_{III} = 222$ nm/RIU. In this case, $fwhm_I = 0.024$, $fwhm_{II} = 0.023$, and $fwhm_{III} = 0.048$, $\Delta\omega_I/\Delta n_I = 0.36$, $\Delta\omega_{II}/\Delta n_{II} = 1.35$, and $\Delta\omega_{III}/\Delta n_{III} = 0.63$. The FoMs of three resonant modes are $\text{FoM}_I = 15.10$, $\text{FoM}_{II} = 57.90$, $\text{FoM}_{III} = 13.19$, respectively. The result shows that mode II is less dependent on the medium into the slit, which means that the air bubbles into the metal slit do not affect the sensitivity of this mode significantly. However, mode I and mode III depend strongly on the media inside the slits. These properties would provide more information about surrounding media when this plasmonic structure is used for sensor applications.

4. Conclusion

In this paper, a novel nanometric plasmonic structure composed of a periodic array of triangular prisms is proposed and its transmission properties are analyzed numerically. When two prisms are combined, novel resonant modes appear in the transmittance spectrum. The influences of the structure parameters, the incident polarization, and the dielectric conditions on the transmission properties are investigated. Results show that several resonant modes appear in the transmission spectra. These resonant modes are less dependent on the incident polarization and depend strongly on the refractive index of surrounding media, which would be very promising for high-sensitivity detection in sensor applications.

Acknowledgments

This work was supported by the National Natural Foundation of China (Grant No. 11004160), the Fundamental Research Funds for the Central Universities

(GK201303007), and the Funds for Undergraduate Students Innovation Training (201310718035).

References

- [1] J.B. Pendry, L. Martin-Moreno, F.J. Garcia-Vidal, Mimicking surface plasmons with structured surfaces, *Science* 305 (2004) 847–848.
- [2] E. Ozbay, Plasmonics: merging photonics and electronics at nanoscale dimensions, *Science* 311 (2006) 189–193.
- [3] A.L. Falk, F.H.L. Koppens, C.L. Yu, K. Kang, N.D. Snapp, A.V. Akimov, M.H. Jo, M.D. Lukin, H. Park, Near-field electrical detection of optical plasmons and single plasmon sources, *Nat. Phys.* 5 (2009) 475–479.
- [4] A.V. Zayats, I.I. Smolyaninov, Near-field photonics: surface plasmon polaritons and localized surface plasmons, *J. Opt. A: Pure Appl. Opt.* 5 (2003) S16–S50.
- [5] K. Lance Kelly, E. Coronado, L.L. Zhao, G.C. Schatz, The optical properties of metal nanoparticles: the influence of size, shape, and dielectric environment, *J. Phys. Chem. B* 107 (2003) 668–677.
- [6] J.B. Lassiter, H. Sobhani, J.A. Fan, J. Kundu, F. Capasso, P. Nordlander, N.J. Halas, Fano resonances in plasmonic nanoclusters: geometrical and chemical tunability, *Nano Lett.* 10 (2010) 3184–3189.
- [7] S. Foteinopoulou, J.P. Vigneron, C. Vandenbem, Optical near-field excitations on plasmonic nanoparticle-based structures, *Opt. Express* 15 (2007) 4253–4267.
- [8] X.F. Fan, W.T. Zheng, D.J. Singh, Light scattering and surface plasmons on small spherical particles, *Light: Sci. Appl.* 3 (2014) 1–14.
- [9] Y.H. Su, Y.F. Ke, S.L. Cai, Q.Y. Yao, Surface plasmon resonance of layer-by-layer gold nanoparticles induced photoelectric current in environmentally-friendly plasmon-sensitized solar cell, *Light: Sci. Appl.* 1 (2012) 1–12.
- [10] Z.Y. Fang, J.Y. Cai, Z.B. Yan, P. Nordlander, N.J. Halas, X. Zhu, Removing a wedge from a metallic nanodisk reveals a Fano resonance, *Nano Lett.* 11 (2011) 4475–4479.
- [11] N. Verellen, Y. Sonnefraud, H. Sobhani, F. Hao, V.V. Moshchalkov, P.V. Dorpe, P. Nordlander, S.A. Maier, Fano resonances in individual coherent plasmonic nanocavities, *Nano Lett.* 9 (2009) 1663–1667.
- [12] M. Piliarik, H. Šípová, P. Kvasnička, N. Galler, J.R. Krenn, J. Homola, High-resolution biosensor based on localized surface plasmons, *Opt. Express* 20 (2012) 672–680.
- [13] L.J. Sherry, S.H. Chang, G.C. Schatz, R.P. Van Duyne, Localized surface plasmon resonance spectroscopy of single silver nanocubes, *Nano Lett.* 5 (2005) 2034–2038.
- [14] S.P. Zhang, K. Bao, N.J. Halas, H.X. Xu, P. Nordlander, Substrate-induced Fano resonances of a plasmonic nanocube: a route to increased-sensitivity localized surface plasmon resonance sensors revealed, *Nano Lett.* 11 (2011) 1657–1663.
- [15] W.L. Barnes, A. Dereux, T.W. Ebbesen, Surface plasmon sub-wavelength optics, *Nature* 424 (2003) 824–830.
- [16] A.R. Zakharian, J.V. Moloney, M. Mansuripur, Surface plasmon polaritons on metallic surfaces, *Opt. Express* 15 (2007) 183–197.
- [17] D.K. Gramotnev, S.I. Bozhevolnyi, Plasmonics beyond the diffraction limit, *Nat. Photonics* 4 (2010) 83–91.
- [18] C.H. Gan, P. Lalanne, Well-confined surface plasmon polaritons for sensing applications in the near-infrared, *Opt. Lett.* 35 (2010) 610–612.

- [19] B.Y. Fan, F. Liu, X.Y. Wang, Y.X. Li, K.Y. Cui, X. Feng, Y.D. Huang, Integrated sensor for ultra-thin layer sensing based on hybrid coupler with short-range surface plasmon polariton and dielectric waveguide, *Appl. Phys. Lett.* 102 (2013) 061109-1–061109-4.
- [20] Z.D. Zhang, H.Y. Wang, Z.Y. Zhang, Fano resonance in a gear-shaped nanocavity of the metal–insulator–metal waveguide, *Plasmonics* 8 (2013) 797–801.
- [21] F. Bahrami, M. Maisonneuve, M. Meunier, J.S. Aitchison, M. Mojahedi, An improved refractive index sensor based on genetic optimization of plasmon waveguide resonance, *Opt. Express* 21 (2013) 20863–20872.
- [22] M. Piliarik, J. Homola, Surface plasmon resonance (SPR) sensors: approaching their limits? *Opt. Express* 17 (2009) 16505–16517.
- [23] Y.Q. Ma, G. Farrell, Y. Semenova, H.P. Chan, H.Z. Zhang, Q. Wu, Sensitivity enhancement for a multimode fiber sensor with an axisymmetric metal grating layer, *Photonics Nanostr. Fundam. Appl.* 12 (2014) 69–74.
- [24] F. Fan, W. Li, W.H. Gu, X.H. Wang, S.J. Chang, Cross-shaped metal–semiconductor–metal plasmonic crystal for terahertz modulator, *Photonics Nanostr. Fundam. Appl.* 11 (2013) 48–54.
- [25] X.P. Zhang, S.F. Feng, T.R. Zhai, Energy transfer channels at the diffraction-anomaly in transparent gratings and applications in sensors, *Photonics Nanostr. Fundam. Appl.* 11 (2013) 109–114.
- [26] K. Tiwari, S.C. Sharma, Surface plasmon based sensor with order-of-magnitude higher sensitivity to electric field induced changes in dielectric environment at metal/nematic liquid–crystal interface, *Sens. Actuators A* 216 (2014) 128–135.
- [27] M. Svedendahl, S. Chen, A. Dmitriev, M. Kall, Refractometric sensing using propagating versus localized surface plasmons: a direct comparison, *Nano Lett.* 9 (2009) 4428–4433.
- [28] P.B. Johnson, R.W. Christy, Optical constants of the noble metals, *Phys. Rev. B* 6 (1972) 4370–4379.
- [29] R.D. Kekatpure, A.C. Hryciw, E.S. Barnard, M.L. Brongersma, Solving dielectric and plasmonic waveguide dispersion relations on a pocket calculator, *Opt. Express* 17 (2009) 24112–24129.
- [30] J.J. Burke, G.I. Stegeman, T. Tamir, Surface-polariton-like waves guided by thin, lossy metal films, *Phys. Rev. B* 33 (1986) 5186–5201.